

Studies on Sublimation of Disperse Dye out of Dyed Polymers. I. Rate of Sublimation and Amorphous Transition Points of Poly(ethylene Terephthalate)

ICHIRO ITO, SABURO OKAJIMA, and FUMIO SHIBATA,
*Fiber and Textile Research Institute, Teijin Limited, Osaka,
Japan, and Faculty of Technology, Tokyo Metropolitan
University, Setagaya-ku, Tokyo, Japan*

Synopsis

Four samples of poly(ethylene terephthalate) film of various crystallinities and orientation were dyed with *p*-nitroaniline and disperse dyes. When these films were heated under a $2-3 \times 10^{-3}$ mm Hg vacuum at a specified temperature T , the dye sublimed out of the dyed specimen. The amount (M_t/M_∞) of sublimed dye is in linear proportion to the square root of the sublimation time, $t^{1/2}$, where M_t and M_∞ are the amounts of dye sublimed for times t and $t = \infty$. The diffusion coefficient D , calculated from the slope of the above plot, is independent of the dye concentration of the film.

When $\log D$ is plotted against $1/T^\circ\text{K}$ over the temperature range 320–520°K, the relation is composed of two to four intersecting lines with the slope decreasing with elevation of temperature and with the breaks at about 89°–98°, 122°–135°, 155° and 175°–176°C. These breaks are the amorphous transitions: the first is the glass transition temperature T_g , the second and the fourth are the amorphous transitions corresponding to the crystalline transition points, i.e., the cold crystallization temperature and the smectic–triclinic transition temperature. With some exceptions, these amorphous transitions are found also by dilatometry and electrical conductivity measurements. The apparent activation energy for diffusion decreases from about 100 kcal/mole for the glass state to 22–24 kcal/mole for the region above 180°C. The activation energy for each region changes slightly with the size of dye molecule and the crystallinity and orientation of the film.

INTRODUCTION

Studies on the correlation between diffusion of penetrants within a polymer and its rheological properties have been published by many authors.¹ However, most studies are limited to amorphous polymers and the molecular size of the penetrants (benzene, acetone, oxygen, hydrogen, nitrogen, etc.) is smaller than, or nearly equal to, that of the structural unit of the polymer. Similar studies also have been carried out in the field of dyeing, for example, on the penetration of disperse dyes into triacetate or diacetate,^{2,3} cationic dyes into polyacrylonitrile,⁴⁻⁷ and acid dyes into nylon.⁸

One of the noticeable results of these studies is that the rate of penetration increases abruptly at T_g but the WLF relation does not always hold good. Another point is that the studies have been focused on a narrow temperature range containing T_g and it is not certain whether or not other amorphous transition points exist between T_g and the melting point of crystalline polymers. Especially in the case of dyeing, the presence of water in the systems to be studied makes it difficult for the experimental technique to be carried out at high temperatures above 100°C and also complicates the system being treated theoretically. However, accumulation of the knowledge of dyeing behaviors at high temperatures above T_g is very important for the technical standpoint of high-temperature dyeing of synthetic fibers.

For these reasons the present authors have established a new method of studying the diffusion behavior of disperse dyes in hydrophobic polymers over wide temperature ranges by measuring (under vacuum) the rate of sublimation of the dye out of the dyed and dried polymer film or filament. The study of such a dry system may possibly contribute to the theoretical analysis of the amorphous region within crystalline polymers at high temperatures because the results obtained can be compared directly with the literature data concerning the fine structure of polymer, which have been obtained usually on dry samples. Another feature of this procedure is its contribution to the knowledge of the fundamental relation between dye sublimation and amorphous structure, which is important not only theoretically but also practically in determining the sublimation fastness of disperse dyes in high-temperature (thermosol) dyeing.

In the present paper, the authors studied the diffusion behavior of disperse dyes in poly(ethylene terephthalate) and found that amorphous transition points exist between T_g and the melting point and that they are related intimately to the crystalline transitions.

EXPERIMENTAL

Samples

Four poly(ethylene terephthalate) films (abbreviated as PET films hereafter) were used as polymer samples (Table I). Four disperse dyes and *p*-nitroaniline (PNA), used as the penetrants, were purified by repeated recrystallization (Table II).

A high-temperature dyeing machine, "Tumblet" (Toa Seiki Ltd., Japan) was used for dyeing. Dyeing temperatures were 70°C (film A, PNA), 90°C (film A, disperse dyes), 100°C (films B and C, PNA), and 120°C (films B and D, disperse dyes). "Disper TL" (anionic surface active agent, registered trade name of Meisei Chemical Works Ltd., Kyoto, Japan) was added to each dye bath at a concentration of 5 g/l. After 3 hr of dyeing, the dyed films were rinsed with cold acetone. It was confirmed that crystallinity of dyed film did not undergo any change by this treatment. The dye

TABLE I
Characterization of PET Films

Film	Characterization
	Inflation film, amorphous and unoriented, 50 μ thick. Supplied by Teijin Ltd.
A	DTA thermogram (10°C/min) indicates a small endothermic and a large exothermic peak at 76° and 131°C cold crystallization, respectively.
B	Commercial "Diafoil" film (Mitsubishi), 12 μ thick. Biaxially oriented and partially crystallized. No remarkable peaks are shown in DTA.
C	Film B was annealed at 220°C for 60 min without restraint.
D	Film A was drawn $\times 5$ and annealed at 200°C for 10 min with the restraint of constant length. Uniaxially oriented and crystallized.

in the film was stripped from the film with monochlorobenzene and then estimated photometrically.

It was confirmed by a spectroscopic method that the dye used did not decompose under the conditions of the following experiments.

Sublimation Apparatus and Experimental Procedures

A sublimation apparatus is shown in Figures 1 and 2. Each 0.0200 g of dyed specimen (I) was placed in a sublimation tube (G), which was immersed in an oil bath (F) controlled at $T^\circ\text{C}$. After preheating for about 5 min, the tap (A) was opened to connect the apparatus to a vacuum line. The dye molecules were sublimed out of the specimen immediately and condensed on the inner surface of the sublimation tube (H) a short distance above the oil surface. Cooling of the tube was accelerated by an air current. After a desired time t , the vacuum was broken by closing the tap A and opening the tap B and the sublimation tube was taken out of the oil bath; the condensed dye was dissolved with monochlorobenzene or an acetone:water 1:1 mixture by volume and estimated spectrometrically. This operation was repeated by varying t . Complete condensation of the sublimed dye was proved within experimental error by correlation with the decrease in dye content of the specimen.

The temperature in the sublimation tube was slightly lower than that of the oil bath; for example, the difference was only 0.4°C when the oil bath temperature was $164 \pm 1^\circ\text{C}$. Hence the sublimation temperature T was indicated by that of the oil bath in the following description.

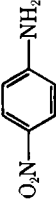

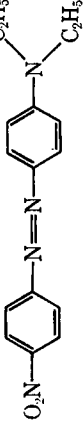
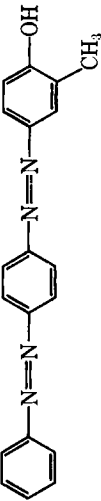
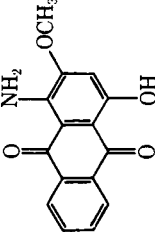
Calculation of Diffusion Coefficient D

Equations (1) and (2) are derived from Fick's diffusion theory for semi-infinite media⁹:

$$M_t = 2(C_0 - C_1)A (D_t/\pi)^{1/2} \quad (1)$$

$$M_t/M_\infty = 2(1 - C_1/C_0)Ad (D_t/\pi)^{1/2} \quad (2)$$

TABLE II
Dye Characteristics

C. I. Disperse	Formula	Purified from
(<i>P</i> -Nitroaniline)		Chemical reagent
Orange 3		Diacelliton F, Orange G
Red 1		Diacelliton Scarlet B
Yellow 7		Kayalon F, Yellow 4R
Red 4		Celliton F, Pink RF

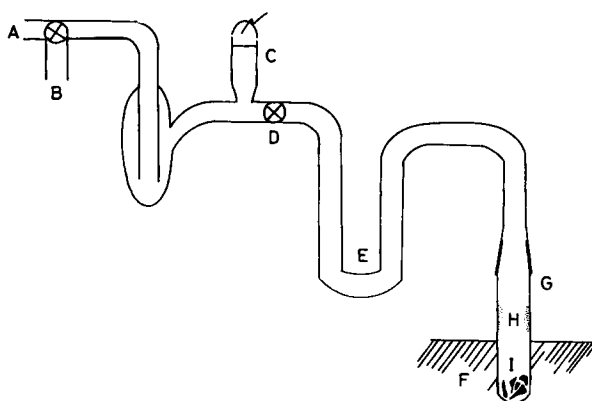


Fig. 1. Schematic diagram of sublimation apparatus: (A) to air; (B) to vacuum pump; (C) vacuum gauge; (D) tap; (E) trap; (F) oil bath; (G) sublimation tube; (H) condensed dye; (I) specimen.

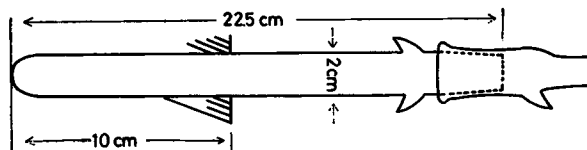


Fig. 2. Details of a sublimation tube.

where M_t = amount of dye, in mg/g specimen, sublimed out of the dyed film at sublimation time t ; M_∞ = value of M_t for $t = \infty$, which is practically equal to the dye content of the specimen; t = sublimation time in min; C_1 = surface concentration of dye, in g/cm³; C_0 = dye concentration of specimen, in g/cm³; A = specific surface of specimen, in cm²/g; D = diffusion coefficient; and d = density of specimen, in g/cm³.

When the pressure p in the sublimation tube decreases, C_1 becomes smaller and therefore the rate of sublimation increases at a certain temperature. Of course the M_t versus $t^{1/2}$ plot shows a linear relation, with the slope increasing as p is reduced progressively, as shown in Figure 3. When the logarithmic value of this slope is plotted against $\log p$, a curve similar to a saturation-type curve is obtained, as indicated in Figure 4. The logarithmic value of the slope almost levels off at values of p below 10^{-2} mm Hg. In this study, p reached $2-3 \times 10^{-3}$ mm Hg within about 1 min after connecting the apparatus to the vacuum line and remained nearly constant thereafter. Therefore D was calculated from eq. (2) under the assumption that C_1/C_0 was negligibly small.

In the case of disperse dyes, the so-called concentration independency of D has been found in the ordinary dyeing of PET from aqueous dye solutions.¹⁰⁻¹² In the case of sublimation out of the dry system, the concentration independency was found as shown in Figure 5, where all the M_t/M_∞ versus $t^{1/2}$ plots coincide independently of the value of M_∞ within experi-

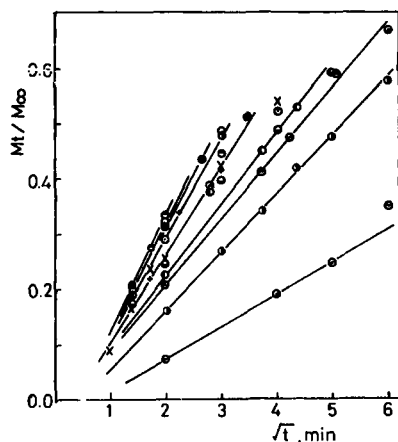


Fig. 3. M_t/M_∞ vs. $t^{1/2}$ plot under various pressures: (\ominus), 0.001 mm Hg (\circ) 0.026 mm Hg; (\bullet) 0.028 mm Hg; (\odot) 0.030 mm Hg; (+) 0.042 mm Hg; (\ominus) 0.050 mm Hg; (\times) 0.056; (\blacklozenge) 0.088 mm Hg; (\oplus) 0.12 mm Hg; (\odot) 0.22 mm Hg; (\odot) 0.60 mm Hg.

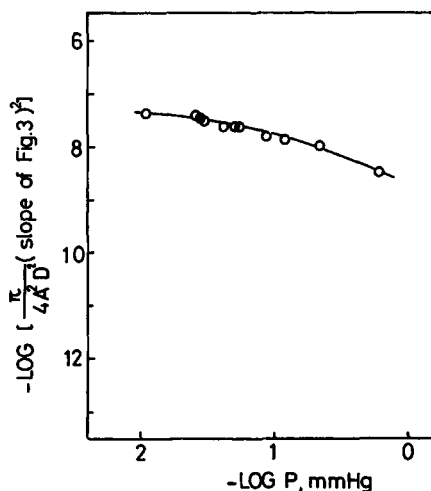


Fig. 4. Relation between the logarithmic value of the slope of Figure 3 and $\log p$.

mental error. A recent study¹³ indicates a steep drop in the value of D at an M_∞ as low as 0–5 mg/g specimen. However, this is only a pseudo-phenomenon because when a correction for the trace of dye remaining unsublimed in the specimen after very long treatment is applied to M_∞ , a constant value of D is always obtained. In the range of M_∞ in the present study, this correction is unnecessary.

Dilatometry

The relative change in polymer volume versus temperature was carried out with an ordinary dilatometer. However, in the case of wet sample, the specially designed dilatometer shown in Figure 6 was used. The rate

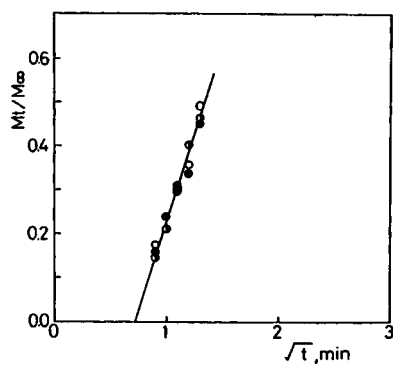


Fig. 5. Effect of dye concentration of film on the plot of M_t/M_∞ vs. $t^{1/2}$. Film B, Red 1, at 181.3°C; (○) $M_\infty = 21.9$; (◐) $M_\infty = 38.2$; (●) $M_\infty = 45.4$ mg/g.

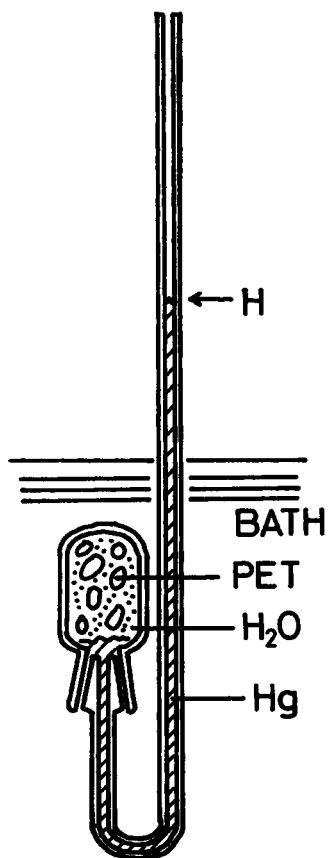


Fig. 6. Dilatometer used for wet sample.

of heating or cooling was $0.5^{\circ}\text{C}/\text{min}$ when the sample was dry, while it was $1^{\circ}\text{C}/\text{min}$ for the wet sample.

Measurement of Electrical Conductivity

The electrical conductivity of PET film was determined with a Takeda Riken vibration reed electrometer type TR-84B, which consisted of two circle electrodes and a guard ring. Aluminum was spattered on both sides of the test film (3.7 cm diameter and $17.1\ \mu$ thick) in order to minimize contact resistance. Resistance was measured with a megohm bridge with the sample in an oven which was controlled to $\pm 1^{\circ}\text{C}$. The test voltage was 92 V dc. From the resistance, the film thickness, and the electrode dimensions, the volume resistivity was calculated from the equation

$$\rho = \frac{\pi d^2}{4t} \cdot Rx$$

where ρ is the resistivity in ohm-cm, Rx is the resistance reading in ohms, d is the diameter of the electrode in cm, and t is film thickness in cm. Volume conductivity, given by the expression $\sigma = 1/\rho$, is expressed in units mho's/cm.

RESULTS AND DISCUSSION

Dye Diffusion and Multitransitions

As a typical example, the plot of M_t/M_{∞} versus $t^{1/2}$ of the film B, dyed with Disperse Red 1, is indicated in Figure 7, where good linearity is ob-

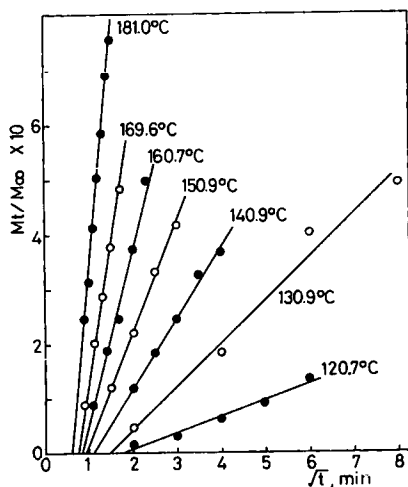


Fig. 7. M_t/M_{∞} vs. $t^{1/2}$ plot of the film B dyed with Disperse Red 1 at various temperatures.

tained for each temperature. However, the lines do not pass through the origin, probably because the dye concentration is not constant throughout the film at $t = 0$ as is required by the basic assumption of eq. (2). That is to say, the concentration just beneath the surface of the film may possibly be lower than that of the inner part as a result of rinsing the dyed film with acetone. Of course, such an abnormal distribution changes gradually during the preheating and the sublimation processes and approaches the theoretical distribution derived from the normal diffusion theory after a certain "induction" time, after which the true linearity holds good. The "induction" time becomes shorter and the intercept of the abscissa decreases as the temperature of sublimation is raised, as seen in Figure 7.

With films dyed with PNA, all the curves pass through the origin. The reason is believed to be that even though the decreased dye concentration just beneath the surfaces does exist at first, the dye distribution becomes rapidly uniform during storage at room temperature or during the preheating of the specimens because of the low molecular weight and high diffusibility of PNA.

Values for D are calculated from the slopes of these lines and their logarithmic values are plotted against the corresponding reciprocal absolute temperatures of sublimation in Figures 8 to 11. It is clearly seen that each plot consists of two, three, or four intersecting lines with decreasing slopes as the temperature is elevated. The breaks in the curves indicate that some transitions occur in the amorphous region at the corresponding temperatures T_{di} ($i = 1, 2, 3$ and 4). As summarized in Table III, the T_{di} values are 89° – 98°C , 126° – 135°C , 155°C and 173° – 176°C for $i = 1, 2, 3$, and 4 , respectively. The value of T_{di} for each film (A to D) is nearly equal for each film, i.e., nearly independent of any difference in orientation or crystallinity, except for T_{di} , which is high in the oriented film and the crystallized film.

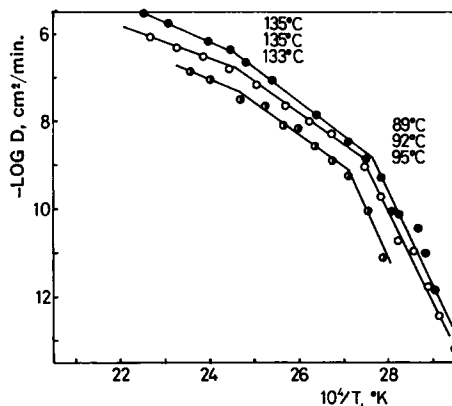


Fig. 8. Diffusion coefficients for PNA: (●) film A; (○) film B; (◐) film C.

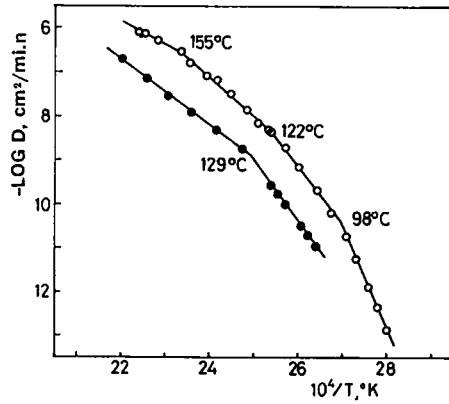


Fig. 9 Diffusion coefficients in film B: (○) C. I. Disperse Orange 3; (●) C. I. Disperse Red 1.

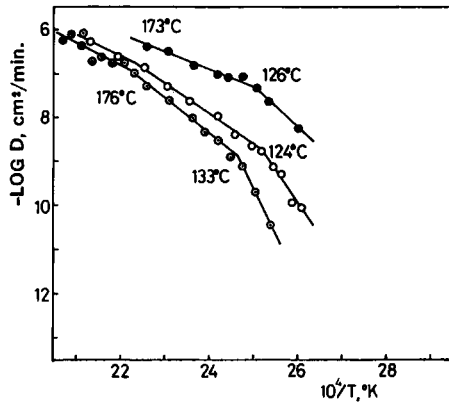


Fig. 10. Diffusion coefficients for C. I. Disperse Yellow 7; (●) film A (○) film B; (◊) film D.

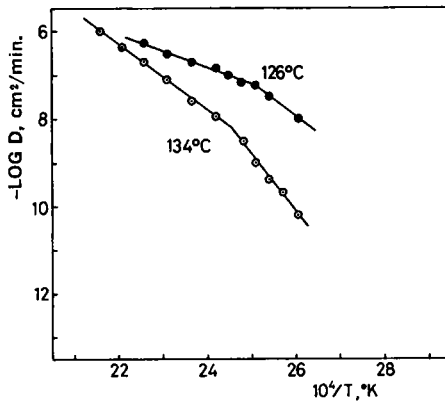


Fig. 11. Diffusion coefficients for C. I. Disperse Red 4; (●) film A; (◊) film D.

TABLE III
Transition Points of Various Dye-Film Systems^a

	Transition point, °C											
	Film A			Film B			Film C			Film D		
	T_{d1}	T_{d2}	T_{d3}	T_{d1}	T_{d2}	T_{d3}	T_{d1}	T_{d2}	T_{d3}	T_{d1}	T_{d2}	T_{d3}
PNA	89	135	—	92	135	—	95	133	—	—	—	—
Orange 3				98	122	155						
Red 1					129	—						
Yellow 7		126	—		124	—	173			133	—	176
Red 4		126	—							134	—	—

^a The spaces indicated by — show no detection of transitions. The blank spaces mean no experiment; some of them are beyond the scope of observation because of the too slow or too rapid sublimation of the dye used.

In the literature only one amorphous transition point has been reported for PET above room temperature and a break in $\log D$ versus $1/T$ plot has been attributed to T_g , while the present authors found three or four breaks in the range 60°–200°C by using a new experimental method which enabled elevation of the upper temperature limit to 200°C. Among the four transition points, T_{a1} can be attributed undoubtedly to T_g , although it is slightly higher than the ordinary T_g value due to orientation and crystallization of the films used.

T_{a2} , ranging from 122° to 135°C is slightly higher than the so-called cold crystallization temperature. T_{a2} might be considered to be due to a change in amorphous region which occurs during cold crystallization. However, this is not correct because T_{a2} also appears in the films C and D, which have been heat treated at 200°C and the crystallites have already rearranged into more complete crystallites than those developed at the cold-crystallization temperature.

According to our view, the amorphous chain segments get sufficient energy near T_{a2} to overcome some restriction. Then a segmental motion of a new mode begins and brings about the cold crystallization. But even above that temperature a fraction of the amorphous segments always remains uncrystallized because they are not in a suitable position to be incorporated into the lattice although they have sufficient energy. Therefore a new thermal motion always begins within the amorphous region when the specimens are heated slightly above the cold-crystallization temperature. This occurs even though the films have been heated at 200°C, because the restriction on the segments from crystallites is overcome at that temperature. This sort of segmental motion ceases reversibly when the temperature is lowered below T_{a2} and appears as the 122°–135°C transition.

As is well known¹⁴ the crystallites developed near T_{a2} are smectic and only (hk0) reflections appear on x-ray photographs. However, the segments in these crystallites rearrange to triclinic lattice above the 180°C and (hkl) patterns appear. This intracrystalline rearrangement is also induced by another new segmental motion in the amorphous region similar to the case of T_{a2} . Hence T_{a4} appears reversibly near 180°C. However, the detailed modes of these segmental motions are not clear at present. According to Nohara¹⁵ and Ito et al.¹⁶ the ethylene group contributes mainly to the segmental motion below T_{a2} and the motion of phenylene groups plays a predominant role above T_{a2} .

The break which appeared at 155°C in film B dyed with Orange 3 is considered to be another transition and is designed as T_{a3} in Table III. (In connection with this point refer to the dilatometry results below.)

Therefore, at least two amorphous transition points are newly found which are considered to be related intimately to the crystalline transition phenomena which have already been found by other authors. However, a few papers have described a transition which can be seen as T_{a2} . In the paper of Fujino et al.¹⁷ on dynamic mechanical properties of Terylene, two $\tan \delta$ peaks (2.4×10^{-2} cps) can be observed at 80°C and 120°C. Helwege

et al.¹⁸ also pointed out two breaks in the volume-versus-temperature plot at 70°C and 120°C. These 120°C transitions seem to correspond to T_{a2} , although the above-mentioned authors have not referred to them. Okajima and Yao¹⁹ and Nakayama and Okajima²⁰ have studied the change of dichroism of dyed polyester film as a function of temperature and found that the dichroism changes discontinuously but reversibly at 120°C. This is also evidence for the existence of T_{a2} . The present authors also tried to furnish further authentication for T_{a2} by other means in the following sections.

At higher temperatures, such as T_{a3} and T_{a4} , reversible partial melting and recrystallization may occur and its effect should be taken into consideration in line with the above-described change in the amorphous region. However, the data in Table IV indicate that the value of the diffusion co-

TABLE IV
Effect of Heat Setting on Diffusion Coefficient of Film D at 125.5°C

Heat setting		D , cm ² /min $\times 10^{10}$
Temp, °C	Time, min	
149.5	12	9.94
179.4	6	10.10
Control		9.88

efficient D at 125.5°C of film D dyed with Yellow 7 does not change by heating to 149.5° or 179.4°C. This suggests that the partial melting is reversible within the limit of the experiment. Of course, the upper temperature limit of this reversibility seems to be a function of the thermal history of the sample. To confirm this point the present authors do not have detailed data at present.

Dilatometry

Dilatometric behavior of the undyed film A and film B dyed with PNA is shown in Figures 12 and 13, respectively. Film A has been quenched, so in the initial heating process (Fig. 12) a small and a large decrease in volume due to the glass transition (70°C) and the cold crystallization (110°–115°C) appear, respectively, in addition to the 156° break. In the cooling process, only two breaks can be seen at 156° and 90°C, the latter being T_g . A second run corresponds to the curve for the cooling process.

In the case of film B, decreases in volume do not appear because it is a commercial product which has probably sustained a heat set; and it was dyed at 100°C, which corresponds to a dry heating at about 120°C. Three breaks can be seen in both the cooling and the heating processes, at 90°–92°, 129°, and 149°–153°C. The plot of the second run agrees with that of the first cooling process, as in the case of film A. Similar results were found for all other films studied. The breaks in the first cooling processes of the various specimens are summarized in Table V.

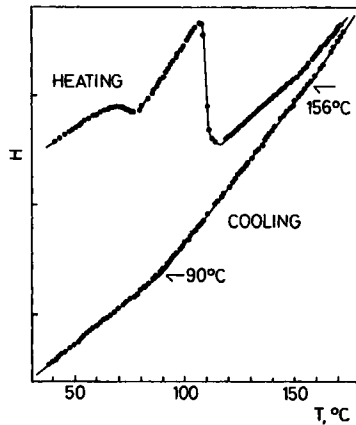


Fig. 12. Dilatometry for film A: 0.5°C/min.

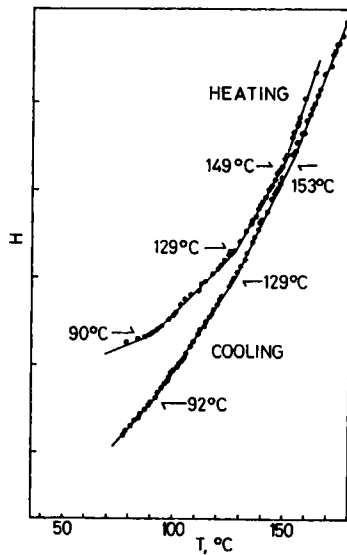


Fig. 13. Dilatometry for film B dyed with PNA.

It is clearly seen from the data in Table V that each film has three breaks, at 87°–95°, 125°–129°, and 153°–157°C, except in the cases of dyed and undyed films A and undyed film B, here the middle break cannot be detected. In general, the break at 125°–129°C is very faint, agreeing with the results of Hellwege et al.⁸ The transitions may possibly exist in these three cases although they are not detected. Of the three breaks, the first two agree well with T_{d1} and T_{d2} . The third does not correspond to T_{d3} but rather to T_{d3} (155°C) of film B dyed with Orange 3 in Table III. It cannot be explained at present why the transition appears clearly in dilatometry but not in the diffusion experiments, except in one case. This remains as a problem for future study.

TABLE V
Breaks in Volume-Versus-Temperature Curves

Film	(1), °C	(2), °C	(3), °C
A	90	—	156
A dyed with PNA	87	—	155
B	90	—	—
B dyed with PNA	92	129	153
C	91	126	157
C dyed with PNA	95	129	153

It is to be expected that the break corresponding to T_{d_1} does not appear in those dilatometry experiments because the temperature is not sufficiently high.

Electrical Conductivity

Warfield and Petree²¹ suggested that measurement of electrical conductivity σ as a function of temperature would provide a convenient method for finding T_g . Barker and Thomas²² found three transitions by applying this method to cellulose acetate. The method is based on the diffusion of ions through the amorphous region in an electric field and the principle is the same as that of our sublimation method.

The plot of $\log \sigma$ versus $1/T$ obtained by the present authors on film D shows the expected transitions at 77° and 110°C (Fig. 14). Of course, the former corresponds to T_{d_1} and the latter to T_{d_2} . The break corresponding to T_{d_2} cannot be detected because of insufficient elevation of T . The apparent activation energy for ion diffusion is 37 kcal/mole above 110°C.

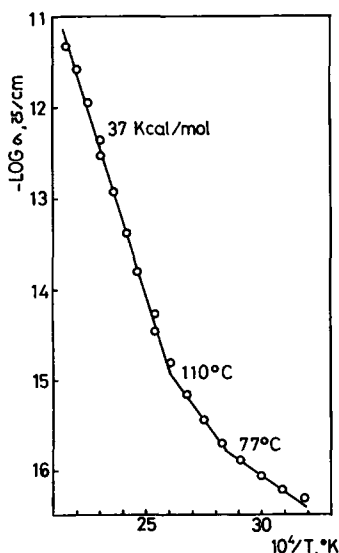


Fig. 14. Electrical conductivity for film D.

Apparent Activation Energy for Diffusion

From the above-mentioned $\log D$ versus $1/T$ plot, the thermal behavior of the amorphous region of PET can be divided into five regions: (1) below T_{d1} ; (2) T_{d1} – T_{d2} ; (3) T_{d2} – T_{d3} ; (4) T_{d3} – T_{d4} ; and (5) T_{d4} and above. Within each region the following equation holds good:

$$D = D_0 \exp \{ -\Delta E/RT \} \quad (3)$$

The apparent activation energy for diffusion, ΔE_i , in the i th region and the frequency factor D_{0i} were calculated and are listed in Tables VI and VII, respectively. Table VI shows that (1) in every film ΔE_i decreases as i increases, irrespective of the size of dye molecule; (2) ΔE_1 and ΔE_2 increase progressively with size of dye molecule; and (3) orientation or crystallization of film has a tendency to increase ΔE_i , which is pronounced in the case of the larger-molecule dyes. However, ΔE_3 does not follow this general tendency and it is noticeable that reversion in the order occurs in the cases where T_{d3} is not detectable (underlined numbers in the table). It may be because these ΔE 's are taking values between ΔE_3 and ΔE_4 .

Cobbs and Burton²³ have studied the relation between crystallization temperature and induction period of crystallization. They have calculated the activation energy of short-distance diffusion of PET segments to be 20 kcal/mole at 120°–170°C, from a consideration that the reciprocal induction period is representing the short-distance diffusion velocity of the segments toward embryos. It is very interesting that ΔE_3 or ΔE_4 of film A is nearly equal to 20 kcal/mole. This suggests that the segmental motion observed by Cobbs and Burton is very similar to that reflected in the diffusion of dyes in the third or fourth region.

It is also noticeable that the apparent activation energy for diffusion of ions is equal to that of dye in the third and fourth region. When the D_{0i} values in Table VII are plotted against the ΔE_i values in Table VI, a linear relationship holds good irrespective of the value of i and the size of dye molecule, as indicated in Figure 15. The data taken from the papers of

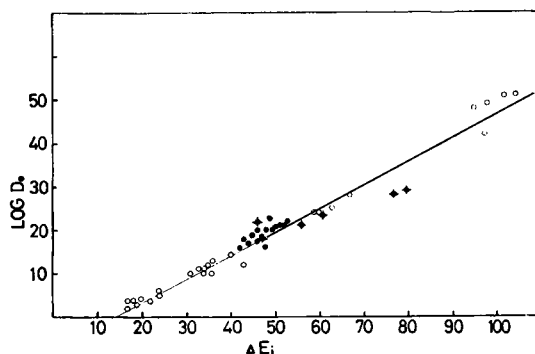


Fig. 15. $\log D_0$ vs. ΔE_i plot for the films A, B, C, and D dyed with various dyes (○): (●) points from Kojima;²⁴ (◆) points from Patterson.

TABLE VI
Apparent Activation Energy for Diffusion

<i>i</i>	Film A					Film B					Film C					Film D				
	1	2	3	4	5	1	2	3	4	5	1	2	3	4	5	1	2	3	4	5
PNA	98	36	20			95	33	17			102	34	19							
Orange 3						104	59	40	24											
Red 1						63		$\frac{34}{31}$			22									
Yellow 7	43		18			67										95		$\frac{36}{34}$		24
Red 4	35		$\frac{17}{17}$													60				

TABLE VII
Logarithmic Frequency Factor

<i>i</i>	Film A					Film B					Film C					Film D				
	1	2	3	4	5	1	2	3	4	5	1	2	3	4	5	1	2	3	4	5
PNA	49	13	4			48	11	2	6		51	11	2							
Orange 3						51	24	14	6											
Red 1						25		$\frac{10}{8}$			4									
Yellow 7	12		2			28										42		10		5
Red 4	12		$\frac{2}{2}$													24		$\frac{10}{10}$		

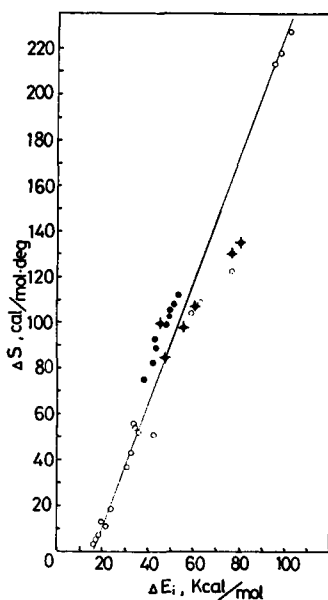


Fig. 16. Relation between ΔS and ΔE ; for films A-B.

Sekido and Kojima^{12,24} also show the same relationship although these data are obtained by dyeing from octane, water, or *n*-butanol solutions at 80°–100°C.

According to Eyring,²⁵ D_0 is expressed by the following equation:

$$D_0 = e\lambda^2 kT/h \exp(\Delta S^\ddagger/R) \quad (4)$$

where λ = jump distance of dye molecule, k = Boltzmann constant, h = Planck constant, R = gas constant, ΔS^\ddagger = entropy of activation for diffusion, and T = absolute temperature of dyeing.

On assuming $\lambda = 15 \text{ \AA}$ after Patterson and Sheldon,² ΔS^\ddagger is calculated from the value of D_0 in Table VII and listed in Table VIII. When these values of ΔS^\ddagger are plotted against the corresponding ΔE in Table VI, the plot can be expressed approximately by a linear relation eq. (5), below, and shown in Figure 16. This is a relation similar to that demonstrated by Meares^{26,27} above T_g for a series of penetrants:

$$\Delta S^\ddagger = 2.53 (\Delta E - 16). \quad (5)$$

Substituting eq. (5) in eq. (4) gives

$$D_0 = 0.54 (\Delta E - 14). \quad (6)$$

In this derivation T is between 350°–440°K and $\log T$ can be considered to be nearly constant. Equation (6) is the line drawn in Figure 15.

ΔS^\ddagger is a function of λ and λ is considered to increase with i . However, the linear relationship between D_0 and ΔE suggests that λ does not change enough to alter the linearity of the relation within experimental error.

TABLE VIII
Entropy of Activation for Diffusion
 ΔS^\ddagger , cal/°K-mole

	Film A					Film B					Film C					Film D						
	i	1	2	3	4	5	1	2	3	4	5	1	2	3	4	5	1	2	3	4	5	
PNA	218	52	13				213	43	4			228	44	7								
Orange 3							226	104	56	19												
Red 1							109		37													
Yellow 7		51		5			122		32	11												
Red 4		48		3																	186	41
																					103	59

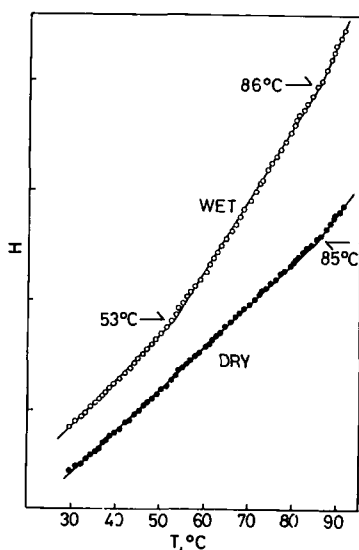


Fig. 17. Dilatometries for film C in dry and wet states.

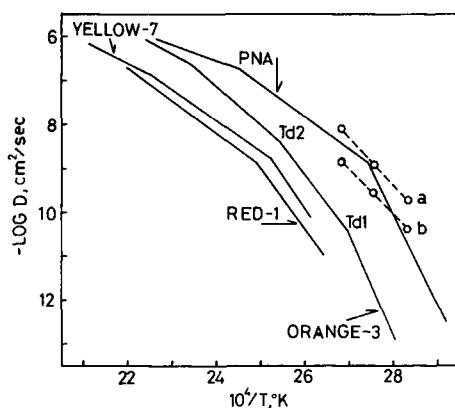


Fig. 18. Diffusion coefficients for various dyes in film B: (a) Mylar and aqueous solutions of Orange 3; (b) Mylar and Red 1. (Lines (a) and (b) are taken from Sekido and Kojima.¹³ The solid lines are taken from Figures 8, 9, and 10.)

Comparison Between Diffusion in Wet and Dry Systems

In practical dyeing, water plays the role of plasticizer for a polymer and shifts the transition points toward the low temperature side. From the results of Fujino et al.²⁸ who have studied the effect of diluents upon the decrease of T_g of PET, it is estimated that only 5 g/kg water absorbed by PET possibly lowers the T_g by about 30°C, providing that the absorbed water has a strong plasticizing action like carriers. Also resiliency versus temperature relation in water shows a 20°C drop of the T_g .^{29,30} A recent study of Nakayama and Okajima³¹ on shrinkage of PET also exhibited a

similar decrease. The results of dilatometry carried out by the present authors on film C in the presence of water showed a break at 53°C, as indicated in Figure 17. This break is probably T_g , because the shift is of the order expected from the above. The dilatometry in the presence of water is so complex that no more can be said about Figure 17.

The diffusion coefficient of dyes in wet PET is extremely large in comparison with those in dry PET, as can be seen in Figure 18. There the dotted lines a and b are the dyeing curves of PET film (Mylar) from aqueous solutions of Orange 3 and Red 1, respectively, reproduced from the paper of Sekido and Kojima¹²; the solid lines are reproduced from Figures 8, 9, and 10 of this paper. The value of $10^4/T_g^\circ\text{K}$ is estimated to be nearly 28 in the wet systems. Since the dotted lines seem to correspond to the solid lines between T_{d1} and T_{d2} of the dry system ($10^4/T^\circ\text{K} = 25-27$), it is suggested that D as well as ΔE are not greatly different in the dry and wet systems.

The extremely larger D of the wet system resulted from the comparison of both systems at the same temperature, i.e., at different rheological regions. However, this is very important from the practical point of view even though it is an apparent phenomenon from the theoretical view point as described above.

References

1. J. Crank and G. S. Park, *Diffusion in Polymers*, Academic Press (1968).
2. E. Iwahori, T. Iijima, and M. Okazaki, *J. Soc. Fiber Science and Techn.*, Japan (Sen-i Gakkaishi), **24**, 118, 300 (1968).
3. B. S. Sprague, *J. Polymer Sci. C*, **20**, 159 (1967).
4. S. Rosenbaum, *J. Appl. Polymer Sci.*, **7**, 1225 (1963); *J. Polymer Sci., A*, **3**, 1949 (1965).
5. T. M. A. Hossain, H. Maeda, and Z. Morita, *J. Polymer Sci., B*, **5**, 1069 (1967).
6. James P. Bell and T. Murayama, *J. Appl. Polymer Sci.*, **12**, 1795 (1968).
7. R. McGregor, R. H. Peters, and C. R. Ramachandran, *J. Soc. Dyers Col.*, **84** 9 (1968).
8. James P. Bell, *J. Appl. Polymer Sci.*, **12**, 627 (1968).
9. J. Crank, *The Mathematics of Diffusion*, Oxford (1956), p. 30.
10. T. G. Majury, *J. Soc. Dyers Col.*, **70**, 442, 445 (1954); **72**, 41 (1956).
11. D. Patterson and R. P. Sheldon, *Trans. Faraday Soc.*, **55**, 1254 (1959).
12. M. Sekido and H. Kojima, *J. Soc. Fiber Science and Techn.*, Japan (Sen-i Gakkaishi), **22**, 33 (1966).
13. Y. Shirakawa and S. Okajima, unpublished.
14. H. G. Kilian, H. Halboth, and E. Jenckel, *Kolloid-Zt.*, **172**, 166 (1960).
15. S. Nohara, *Chemistry of High Polymers*, Japan, **14**, 318 (1957).
16. E. Ito, R. Hatakeyama, A. Koyama, H. Kanetsuna, and S. Okajima, *Kogyo Kagaku Zasshi*, **72**, 2318 (1969).
17. K. Fujino, N. Fujimoto, and K. Eto, *J. Textile Machinery Soc.*, Japan, **14**, 291 (1961).
18. K. H. Hellwege, J. Hennig, and W. Knappe, *Kolloid-Zt.*, **186**, 29 (1962).
19. S. Okajima and S. Yao, *J. Soc. Fiber Science and Techn.*, Japan (Sen-i Gakkaishi), **22**, 17 (1966).
20. K. Nakayama, S. Okajima, and K. Kobayashi, *J. Appl. Polymer Sci.*, **13**, 659 (1969).

21. R. W. Warfield and M. C. Petree, *Polymer*, **1**, 178 (1960); *SPE Trans.*, **1**, 1 (1960); *Makromol. Chem.*, **58**, 139 (1962).
22. R. E. Barker and C. R. Thomas, *J. Appl. Phys.*, **35**, 87 (1964).
23. W. H. Cobbs and R. L. Burton, *J. Polymer Sci.*, **10**, 275 (1953).
24. H. Kojima, *Kogyo Kagaku Zasshi*, **70**, 183 (1967).
25. S. Glasstone, H. Eyring, and K. T. Laidler, *Theory of Rate Process* (1941).
26. P. Meares, *J. Am. Chem. Soc.*, **76**, 3415 (1954).
27. P. Meares, *Trans. Faraday Soc.*, **53**, 101 (1957).
28. K. Fujino, N. Kuroda, and F. Fujimoto, *J. Soc. Fiber Science and Techn.*, Japan (Sen-i Gakkaishi), **21**, 573 (1965).
29. C. M. Bryant and A. T. Walter, *Textile Res. J.*, **29**, 211 (1959).
30. A. Brown, *Textile Res. J.*, **25**, 891 (1955).
31. S. Okajima and K. Nakayama, unpublished.

Received October 13, 1969